Appl Phys B (2012) 106:379–384
DOI 10.1007/s00340-011-4746-2

Applied Physics B
Lasers and Optics

Cross-validation of theoretically quantified fiber continuum generation and absolute pulse measurement by MIIPS for a broadband coherently controlled optical source

H. Tu · Y. Liu · J. Lægsgaard · D. Turchinovich · M. Siegel · D. Kopf · H. Li · T. Gunaratne · S.A. Boppart

Received: 11 May 2011 / Revised version: 27 June 2011 / Published online: 11 October 2011

Abstract The predicted spectral phase of a fiber continuum pulsed source rigorously quantified by the scalar generalized nonlinear Schrödinger equation is found to be in excellent agreement with that measured by multiphoton intrapulse interference phase scan (MIIPS) with background subtraction. This cross-validation confirms the absolute pulse measurement by MIIPS and the transform-limited compression of the fiber continuum pulses by the pulse shaper performing the MIIPS measurement, and permits the subsequent coherent control on the fiber continuum pulses by this pulse shaper. The combination of the fiber continuum source with the MIIPS-integrated pulse shaper produces compressed transform-limited 9.6 fs (FWHM) pulses or arbitrarily shaped pulses at a central wavelength of 1020 nm, an average power over 100 mW, and a repetition rate of 76 MHz. In comparison to the 229-fs pump laser pulses that generate the fiber continuum, the compressed pulses reflect a compression ratio of 24.

H. Tu (✉) · Y. Liu · S.A. Boppart
Biophotonics Imaging Laboratory, Beckman Institute for Advanced Science and Technology, University of Illinois at Urbana-Champaign, Urbana, IL 61801, USA
e-mail: htu@illinois.edu

S.A. Boppart
e-mail: boppart@illinois.edu

J. Lægsgaard · D. Turchinovich
DTU Fotonik—Department of Photonics Engineering, Technical University of Denmark, 2800 Kgs. Lyngby, Denmark

M. Siegel · D. Kopf
High Q Laser Innovation GmbH, Feldgut 9, 6830 Rankweil, Austria

H. Li · T. Gunaratne
BioPhotonics Solutions, Inc., 1401 East Lansing Drive, Suite 112, East Lansing, MI 48823, USA

1 Fiber continuum pulsed source with theoretically quantified temporal field

Broadband coherently controlled optical sources with transform-limited (TL) pulse compression and arbitrary pulse shaping by a spatial light modulator (SLM)-based $4f$ pulse shaper [1] are in strong demand for spectroscopy and microscopy applications [2–5]. The single most representative example of these sources is the ultra-broadband Ti:sapphire oscillator [6], which has been commercially available for many years. However, this oscillator source limits the emission band to 700–1000 nm (typically), and is prone to small alignment drifts in the laser cavity that can lead to high maintenance cost. An alternative source is the fiber continuum generated by pumping a nonlinear optical fiber with a regular narrow-band laser oscillator [7, 8]. Unfortunately, most fiber continuum sources have insufficient coherence to allow efficient pulse compression [9], let alone TL compression, and are therefore not useful for coherent control applications. For a brief review of the available compressible fiber continuum sources, we refer to Table 1 in [8] and the references therein.

Among the compressible fiber continuum sources, the solid-state Yb laser-pumped fiber continuum developed recently [8] appears to be a practical alternative to the ultra-broadband Ti:sapphire oscillator in terms of broad bandwidth (880–1180 nm), average power (361 mW), pulse energy (4.7 nJ), and spectral power density (∼1 mW/nm). More importantly, the fully known temporal field (amplitude and phase, either temporal or spectral) of this fiber continuum can guide the pulse compression, just like that of a

well-aligned ultra-broadband Ti:sapphire oscillator generating TL pulses with constant spectral phase. Since the distinctly structured spectrum of this Yb laser-pumped fiber continuum has been accurately predicted from the temporal field of the fiber continuum pulses by the scalar generalized nonlinear Schrödinger equation (GNLSE), the corresponding spectral phase of the pulses has been theoretically predicted with high confidence [8].

In order to achieve TL pulse compression in the context of microscopy, we have used a SLM to remove the combined linear and nonlinear chirps from this fiber continuum and the corresponding transmitting optics [10]. However, it is of theoretical and practical interest to experimentally validate the spectral phase associated with the fiber continuum only (and the corresponding nonlinear fiber-optics simulation by the scalar GNLSE), to compensate the spectral phase by a well-calibrated SLM-based $4f$ pulse shaper, and to perform arbitrary pulse shaping by the pulse shaper thereafter. To construct this coherently controlled fiber continuum source, a dedicated pulse measurement instrument, e.g., frequency-resolved optical gating (FROG) [11], or spectral phase interferometry for direct electric-field reconstruction (SPIDER) [12], is usually required for the initial setup and daily maintenance. This adds considerable complexity and cost to the source so that laser experts are needed for routine operations. It is our main objective in this study to implement such coherently controlled fiber continuum source without introducing additional hardware. The necessary pulse measurement to validate the spectral phase is conducted by the $4f$ pulse shaper itself, using the procedure of multiphoton intrapulse interference phase scan (MIIPS) [13, 14].

2 Scheme for absolute pulse measurement by MIIPS

MIIPS is an ultrashort pulse technique that simultaneously measures and shapes femtosecond (fs) laser pulses using an adaptive pulse shaper. Conventional ultrashort pulse techniques such as autocorrelation, FROG, and SPIDER can only measure the pulse characteristics. Two recent papers have reviewed the ultrashort ($\sim$10 fs) pulse measurement and shaping by MIIPS [13, 14]. In term of pulse measurement, the fundamental difference between MIIPS and FROG (or SPIDER) employing all-reflective dispersion-free optics is that a $4f$ pulse shaper must be inserted into the beam path of the pulses to assist with the pulse measurement. Unfortunately, the pulse shaper itself may not be dispersion-free, so that the measured spectral phase of the pulses represents the contribution from the pulses themselves (signal) and that from the $4f$ pulse shaper (background). In other words, MIIPS measures the pulses after (and possibly modified by) the $4f$ pulse shaper, rather than the original pulses before the $4f$ pulse shaper. In this sense, the pulse measurement by FROG or SPIDER is "absolute" (or "background-free"), while that by MIIPS is "relative" (or "differential"). This aspect of MIIPS, together with the strict calibration requirement of the SLM in the $4f$ pulse shaper for accurate phase retrieval, may contribute to the perceived limitations of the MIIPS measurement.

Intuitively, the absolute pulse measurement by MIIPS can be realized by subtracting this background, which can be measured by linear spectral interferometry [15]. However, in order to strictly test the pulse measurement and compression by MIIPS, we choose to send repetitive TL pulses into the $4f$ pulse shaper and perform MIIPS on the pulses right after the $4f$ pulse shaper. The required TL pulses are generated by compressing the pulses to be measured by an auxiliary MIIPS-integrated $4f$ pulse shaper, which is not needed once the background has been measured (Fig. 1(a)–1(c), see details below).

To validate this relatively unknown capability of the absolute pulse measurement by MIIPS, a "reference" pulsed source with fully known temporal field is required. Here we test the potential of the above fiber continuum as such reference. We find that the spectral phase of the fiber continuum pulses obtained by this absolute pulse measurement is in excellent agreement with that calculated from the scalar GNLSE. Since neither the theoretically quantified fiber continuum generation nor the absolute pulse measurement by MIIPS has been independently validated, we term this unusual agreement a "cross-validation".

3 Regular measurement, compression, and shaping of fiber continuum pulses by MIIPS

Our fiber continuum was generated by launching the 1040-nm 229-fs (FWHM) 76-MHz pulse from a diode-pumped solid-state Yb:KYW laser (FemtoTRAIN, High-Q laser GmbH, Austria) into the 2.3 μm core of a 91-mm all-normal dispersion non-birefringent photonic crystal fiber (NL-1050-NEG-1, Crystal Fibre A/S, Denmark) [8]. We used a short-focal-length (5 mm) 90° off-axis parabolic mirror to collimate the fiber continuum output into a $\sim$2.5 mm-diameter beam. A commercial beam profiler was employed to ensure high quality collimation over long distances (10–20 m). The fiber continuum source had a central wavelength of 1020 nm, an average power of 361 mW, a pulse repetition rate of 76 MHz, and a largely horizontal polarization with a polarization extinction ratio of 20. The optical frequency-dependent spectrum of the fiber continuum source is shown in Fig. 2(a), which is derived from the wavelength-dependent spectrum reported previously [8]. Despite the highly structured profile, the spectrum along with the average power (361 mW) of the fiber continuum source remains stable after $>$100 hrs of operation. This is

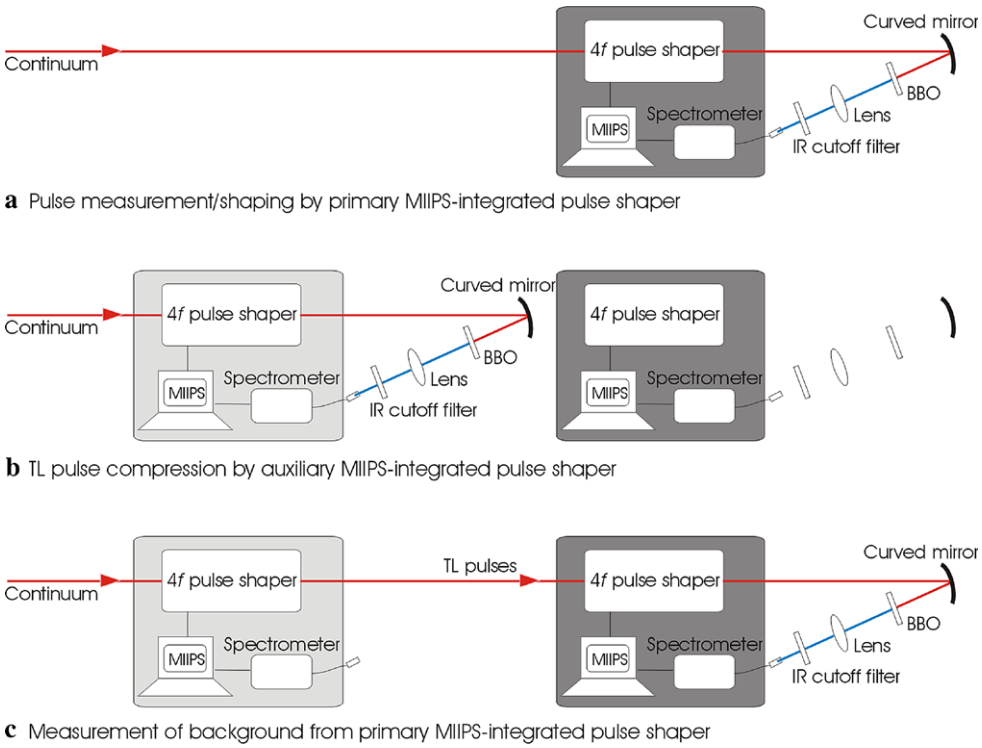

Fig. 1 Scheme for absolute pulse measurement by MIIPS. The background of the pulse measurement by the primary MIIPS-integrated pulse shaper (**a**) is obtained by the pulse compression in (**b**) and the subsequent measurement in (**c**) with the assistance of an auxiliary MIIPS-integrated pulse shaper

perhaps not surprising because this measured spectrum and its unknown spectral phase have been deterministically predicted by the scalar GNLSE with relatively few parameters (Fig. 2(a)–2(b)) [8].

The collimated fiber continuum was then sent to a commercial MIIPS-integrated 4f pulse shaper (MIIPS Box640, BioPhotonicSolutions, Inc., East Lansing, MI) designed for broadband (700–1350 nm) operation on a 640-pixel SLM, corresponding to a spectral resolution of ~1 nm/pixel (Fig. 1(a)). The SLM can perform both phase and amplitude shaping. However, only phase shaping was carried out in this study. A curved mirror ($f = 100$ mm) focused the output beam from the pulse shaper onto a 10 μm thick BBO crystal, while the resulting second-harmonic generation (SHG) signal was collected by a lens ($f = 100$ mm) and guided into a fiber-coupled spectrometer. The SHG signal served as the necessary feedback for the MIIPS procedure. The average power of the fiber continuum at the focus of the curved mirror was 110 mW (measured by replacing the BBO crystal with a power meter), corresponding to a throughput of 30% for the pulse shaper. Similarly, the spectrum of the fiber continuum at the focus of the curved mirror was measured by an optical spectrum analyzer, and was similar to that of the fiber continuum source (Fig. 2(c)). The small difference might be attributed to the wavelength-dependent diffraction efficiency and the polarization filtering of the pulse shaper.

The spectral phase of the fiber continuum pulses after the pulse shaper (uncompressed pulses) was successfully retrieved by standard MIIPS procedure and subsequently compensated by the pulse shaper, resulting in phase-compensated (compressed) pulses with a small uncompensated residual spectral phase across the bandwidth of the fiber continuum (Fig. 2(b)). The reconstructed temporal intensity profile of the compressed pulses approximates that of the TL pulses (with zero spectral phase) obtained from the spectrum (after shaper) of Fig. 2(c) (Fig. 2(d)). In repeated pulse compression experiments, the FWHM pulse width of the compressed pulses is only slightly (<2%, typically) larger than that of the TL pulses. This ability of TL pulse compression is indicative of the high-precision spectral phase measurement by MIIPS [14]. The SHG spectra corresponding to the uncompressed and compressed pulses were recorded immediately before and after the electronically-driven phase compensation, without varying any other experimental parameters. The effectiveness of the pulse compression is represented by a 32-fold increase of the integrated SHG intensity (over frequency) after the phase compensation (Fig. 2(e)–2(f), note the different vertical scales).

To quantitatively understand this result, we calculate the SHG spectrum according to $S(2\omega) = |\int |E(\omega+\Omega)| \times e^{i\varphi(\omega+\Omega)} |E(\omega-\Omega)| e^{i\varphi(\omega-\Omega)}\, d\Omega|^2$, where Ω is integrated over the fiber continuum spectrum [12]. The amplitude components in the integral are derived from the measured fiber continuum spectrum (Fig. 2(c)) with proper scaling, while the exponentials in the integral are either treated as unity for TL pulses (Fig. 2(f)) or calculated according to the retrieved

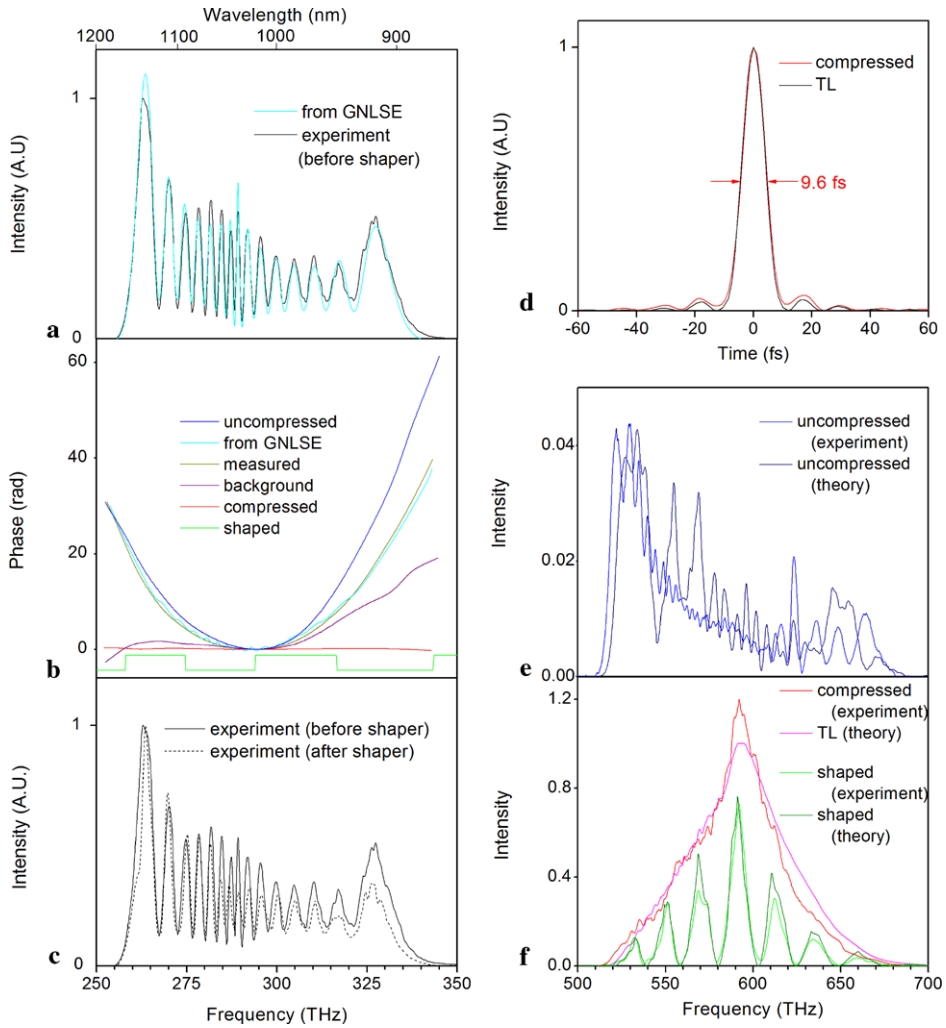

Fig. 2 (**a**) Measured spectrum of fiber continuum source and the scalar GNLSE-quantified spectrum. (**b**) Comparison of the spectral phases corresponding to the uncompressed pulses, the scalar GNLSE-quantified fiber continuum pulses, the measured pulses, the background of the MIIPS-integrated pulse shaper, the compressed pulses, and the shaped pulses (see details in text). (**c**) Comparison of measured spectrum of fiber continuum source (before shaper) and measured spectrum of fiber continuum at the focus of the curved mirror (after shaper). (**d**) Reconstructed temporal profiles of the compressed pulses and the corresponding TL pulses. (**e**) Comparison of the measured and calculated SHG spectra of the uncompressed pulses. (**f**) Comparison of the measured SHG spectrum of the compressed pulses and the calculated SHG spectrum of the TL pulses, and of the measured and calculated SHG spectra of the shaped pulses

spectral phase of the uncompressed pulses (Fig. 2(e)). The calculated SHG spectrum of the uncompressed pulses is found to be in good agreement with its experimental counterpart (Fig. 2(e)), while the calculated SHG spectrum of the TL pulses approximates that of the observed SHG spectrum of the compressed pulses (Fig. 2(f)). The enhancing factor of the calculated integrated SHG intensity due to full phase compensation is found to be 31, which also agrees well with the experimental value of 32. As a final test, a binary $(0, \pi)$ phase mask was introduced on the SLM in the $4f$ pulse shaper after the phase compensation, or equivalently, this binary phase mask was superimposed on the residual phase of the compressed pulses to produce specific shaped pulses (Fig. 2(b)), and the SHG spectrum of the shaped pulses was recorded (Fig. 2(f)). Again, this recorded SHG spectrum agrees well with the theoretically calculated spectrum corresponding to the spectral phase of the shaped pulses (Fig. 2(f)). This evidence strongly justifies the pulse measurement and the TL pulse compression by MIIPS, and the arbitrary coherent control on the fiber continuum source.

4 Cross-validation by measuring the background from MIIPS-integrated pulse shaper

The above SHG analysis justifies the reliable pulse measurement and the TL pulse compression by MIIPS, and allows the following measurement of the background spectral phase introduced by the (primary) MIIPS-integrated $4f$ pulse shaper to the fiber continuum source (Fig. 1(a)). First, an auxiliary MIIPS-integrated $4f$ pulse shaper similar to the primary pulse shaper was inserted into the beam path of the primary pulse shaper to generate TL fiber continuum pulses by MIIPS (Fig. 1(b)). The TL fiber continuum pulses were then sent to the primary pulse shaper, and the background spectral phase (Fig. 2(b)) was readily measured by performing MIIPS in the primary pulse shaper (Fig. 1(c)). The spectral phase of the fiber continuum source from the absolute measurement by MIIPS was obtained by subtracting this background from the spectral phase of the uncompressed pulses (Fig. 2(b)). Extraordinarily, the measured spectral phase is in excellent agreement with that of the fiber continuum source calculated by the scalar GNLSE (Fig. 2(b)).

In contrast to the SHG analysis that validates the MIIPS-retrieved spectral phase rather indirectly, this coincidence (i.e., cross-validation) validates the MIIPS-retrieved spectral phase directly, and therefore more strongly confirms the pulse measurement, compression, and shaping by MIIPS as described above.

The background spectral phase may be attributed to the dispersion of the liquid-crystal SLM mask and its built-in polarizer at the Fourier plane of the $4f$ pulse shaper. The other optical components of the MIIPS-integrated $4f$ pulse shaper were reflective and were aligned to be dispersion-free [1]. Once the background has been measured, the absolute measurement by MIIPS takes the form of Fig. 1(a), so that the auxiliary pulse shaper is no longer needed. The spectral phase of the fiber continuum source has been consistently measured in repeated measurements, with statistical phase errors smaller than the difference between the measured and the scalar GNLSE-quantified spectral phases in Fig. 2(b) [13].

5 Remarks on performance of MIIPS-enhanced fiber continuum source

Only one MIIPS-integrated $4f$ pulse shaper that has been "background subtracted" is required for each coherently controlled source (Fig. 1(a)). This background subtraction (Fig. 1(a)–1(c)) is routinely done in the factory before the MIIPS-integrated $4f$ pulse shaper is shipped. The MIIPS-enhanced fiber continuum source (880–1180 nm) competes well with the dominant coherently controlled source combining an ultra-broadband Ti:sapphire oscillator with a regular $4f$ pulse shaper. First, the broad spectrum and spectral phase of the fiber source is stabilized only by controlling the fiber launching efficiency, in contrast to the Ti:sapphire laser that relies heavily on strict optical alignment to mode-lock a broad bandwidth. This implies an improved robustness, long-term stability, and user friendliness of the fiber source. Second, the solid-state pump Yb laser of the fiber source is a directly diode-pumped, air-cooled, compact (head dimension $8 \times 6 \times 52$ cm) laser with turnkey maintenance-free operation, while the fiber launcher of the fiber source is a compact passive optical device. Thus, the fiber source is more suitable for portable applications such as clinical biomedical imaging. Third, the MIIPS procedure eliminates the collinear two-beam interferometer setup of SPIDER and FROG for separate pulse measurement. The MIIPS-enhanced fiber continuum source integrates the absolute pulse measurement and the pulse compression/shaping into a single-beam interferometer-free setup (Fig. 1(a)), resulting in the maximum experimental simplicity and minimum cost for targeted delivery of arbitrarily coherently controlled pulses. Fourth, the fiber continuum is generated in an all-normal dispersion fiber so that small relative intensity noise [16] and excellent coherence [17] are expected. Finally, the fiber source appears to have good long-term stability. To date, the power and the spectrum of the source have remained stable for over 200 hours of operation. We believe this source is operating well below the photo-damage threshold of silica glass.

It should be noted that the limited bandwidth of the Yb gain medium has restricted the pulse duration to >50 fs for solid state systems [18], or >28 fs for fiber-based systems with somewhat degraded spectral-temporal performance [19]. The generated 9.6-fs TL pulses in this study are to our knowledge the shortest pulses for Yb-based sources. In addition, the compressed 9.6-fs TL pulses represent a compression ratio of 24 in comparison to the 229-fs pump laser pulses employed in the continuum generation, which we believe is currently the largest compression ratio for sub-10 fs pulse compression of fiber continuum. The high performance of this fiber source can be attributed to the proper choice of a fiber dispersion profile for a given pump wavelength, so that highly coherent continuum can be generated. The parameter space of the pump wavelength and the dispersion of the fiber to achieve similar performance have been discussed in a previous paper [8]. We note that the Er:fiber laser-pumped fiber continuum (980–1400 nm) developed by Leitenstorfer and co-workers has similar advantages over the ultra-broadband Ti:sapphire oscillator, and has been compressed to an impressive (but not TL) pulse duration of 7.8 fs [20]. Also, the Ti:sapphire laser-pumped fiber continuum (740–880 nm) developed by Motzkus and co-workers has been compressed to near TL pulses of 14.4 fs [21, 22].

6 Conclusions

A MIIPS-enhanced fiber continuum source centered at 1020 nm has been developed as an effective and attractive broadband coherently controlled source. The construction of this source involves only commercial components, while the performance of the source competes well with an ultra-broadband Ti:sapphire oscillator. This source has strongly demonstrated the predictability and reliability needed to control the fiber continuum, and is potentially useful for multiphoton microscopy and coherent control microspectroscopy.

Acknowledgements This work was supported by grants from the National Institutes of Health (NCI R33 CA115536; NIBIB R01 EB009073; NCI RC1 CA147096, S.A.B.), and from the Danish Council for Independent Research—Technology and Production Sciences (FTP). Additional information can be found at http://biophotonics.illinois.edu.

References

1. A.M. Weiner, Rev. Sci. Instrum. **71**, 1929 (2000)
2. V.V. Lozovoy, M. Dantus, Chem. Phys. Chem. **6**, 1970 (2005)
3. Y. Silberberg, Annu. Rev. Phys. Chem. **60**, 277 (2009)
4. B. von Vacano, M. Motzkus, in *Biochemical Applications of Nonlinear Optical Spectroscopy*, ed. by V.V. Yaokovlev (CRC Press, Boca Raton, 2009), pp. 167–196
5. K. Isobe, M. Tanaka, F. Kannari, H. Kawano, H. Mizuno, A. Miyawaki, K. Midorikawa, IEEE J. Sel. Top. Quantum Electron. **16**, 767 (2010)
6. U. Morgner, F.X. Kärtner, S.H. Cho, Y. Chen, H.A. Haus, J.G. Fujimoto, E.P. Ippen, V. Scheuer, G. Angelow, T. Tschudi, Opt. Lett. **24**, 411 (1999)
7. J.K. Ranka, R.S. Windeler, A.J. Stentz, Opt. Lett. **25**, 25 (2000)
8. H. Tu, Y. Liu, J. Lægsgaard, U. Sharma, M. Siegel, D. Kopf, S.A. Boppart, Opt. Express **18**, 27872 (2010)
9. J.M. Dudley, G. Genty, A. Coen, Rev. Mod. Phys. **78**, 1135 (2006)
10. H. Tu, Y. Liu, D. Turchinovich, S.A. Boppart, Opt. Lett. **36**, 2315 (2011)
11. R. Trebino, *Frequency-Resolved Optical Gating: The Measurement of Ultrashort Laser Pulses* (Kluwer Academic, Dordrecht, 2002)
12. C. Iaconis, I.A. Walmsley, Opt. Lett. **23**, 792 (1998)
13. B. Xu, J.M. Gunn, J.M. Dela Cruz, V.V. Lozovoy, M. Dantus, J. Opt. Soc. Am. B **23**, 750 (2006)
14. Y. Coello, V.V. Lozovoy, T.C. Gunaratne, B. Xu, I. Borukhovich, C. Tseng, T. Weinacht, M. Dantus, J. Opt. Soc. Am. B **25**, A140 (2008)
15. L. Lepetit, G. Chériaux, M. Joffre, J. Opt. Soc. Am. B **12**, 2467 (1995)
16. N. Nishizawa, J. Takayanagi, J. Opt. Soc. Am. B **24**, 1786 (2007)
17. A.M. Heidt, J. Opt. Soc. Am. B **27**, 550 (2010)
18. M. Tokurakawa, A. Shirakawa, K. Ueda, H. Yagi, M. Noriyuki, T. Yanagitani, A.A. Kaminskii, Opt. Express **17**, 3353 (2009)
19. X. Zhou, D. Yoshitomi, Y. Kobayashi, K. Torizuka, Opt. Express **16**, 7055 (2008)
20. A. Sell, G. Krauss, R. Scheu, R. Huber, A. Leitenstorfer, Opt. Express **17**, 1070 (2009)
21. B. von Vacano, T. Buckup, M. Motzkus, J. Opt. Soc. Am. B **24**, 1091 (2007)
22. B. von Vacano, T. Buckup, M. Motzkus, Opt. Lett. **31**, 1154 (2006)